

Fourth Quarterly Report
for

SOLAR CELL COVER GLASS DEVELOPMENT

(1 May 1967 through 1 October 1967)

Contract Number: NAS5-10236

Prepared by:

Ion Physics Corporation
Burlington, Massachusetts

Prepared for:

Goddard Space Flight Center
Greenbelt, Maryland

N68-36241
(ACCESSION NUMBER)
62 (PAGES)
CP-97123
(NASA CR OR TMX OR AD NUMBER)

(THRU)
1
(CODE)
03
(CATEGORY)

FACILITY FORM 602

GPO PRICE \$ _____

CSFTI PRICE(S) \$ _____

Hard copy (HC) _____

Microfiche (MF) _____

ff 653 July 65

ION PHYSICS CORPORATION

A Subsidiary of High Voltage Engineering Corporation

BURLINGTON, MASSACHUSETTS



Quarterly Technical Progress Report No. 4

1 May 1967 through 1 October 1967

SOLAR CELL COVER GLASS DEVELOPMENT

National Aeronautics and Space Administration
Goddard Space Flight Center
Greenbelt, Maryland

Contract NAS5-10236

Project Engineer: Roger W. Sudbury
R. W. Sudbury

ION PHYSICS CORPORATION
BURLINGTON, MASSACHUSETTS

OBJECTIVE

The objective of this program is refinement and economic optimization of techniques for fabrication of thick integral coverslips for silicon solar cells. An a priori assumption is that integral coverslip cells must show a definite superiority over conventional glued coverslip cells. The consequences of this assumption provide natural guidelines for selection of candidate coverslip materials, possible fabrication techniques and environmental test end points. Specifically, all coverslip materials that are known to significantly degrade under ultraviolet, proton or electron irradiation must be categorically excluded from consideration. Similarly, all fabrication techniques that are inherently deleterious to the cell structure itself must be rejected. Finally, the environmental and radiation test end points must be at least as severe as those encountered with glued coverslip cells. For ease in comparison, final testing is to be done on cells with 6 mil integral coverslips.

FOREWORD

This report was prepared by Ion Physics Corporation, Burlington, Massachusetts, under National Aeronautics and Space Administration, Goddard Space Flight Center, Contract NAS5-10236. It is a Technical Progress Report and covers the period 1 May 1967 through 1 October 1967.

The chief contributors and their fields of interest are:

	<u>Staff Function</u>	<u>Program Area</u>
Dr. W. J. King	Vice President Director, Solid State Division	
S. J. Solomon	Senior Scientist	
R. W. Sudbury	Group Leader	Project Engineer
S. Harrison	Group Leader	Optical Coatings
A. Kirkpatrick	Physicist	Coverslipping
K. Stirrup	Physicist	Contacts
J. T. Burrill	Production Manager	Cell Fabrication

SUMMARY

Ion Physics Corporation's proprietary high vacuum sputtering process has been shown to be well suited to the deposition of integral SiO_2 coverslips onto silicon solar cells. Since, however, this process has a rate limitation and the deposited SiO_2 is stressed, it is important to examine other processes that could more quickly deposit less stressed SiO_2 over an initial high vacuum sputtered layer. Both reactive sputtering and electron beam evaporation have been investigated as a means of building up coverslip thickness. To date, it has not yet been possible to deposit satisfactory thick layers of SiO_2 by either of these processes.

Reactively sputtered SiO_2 layers are hard and well bonded, but thick films suffer from physical and optical inhomogeneities and cannot yet be considered acceptable for integral coverslip cells. The problem is thought to be associated with backscattering of SiO_2 onto the Si cathode and subsequent dispersion of this SiO_2 in fragment form. Investigation is continuing and it is anticipated that these problems may be solved by conversion of the present dc apparatus to an RF or RF plus dc system.

Although electron beam evaporated SiO_2 is well bonded, it is invariably of poor physical quality. Since similar soft, 'frothy' material has been produced not only by IPC but by outside vendors as well, this approach has been discontinued. The properties of Al_2O_3 suggest it may be a better possibility for electron beam evaporation and effort is now to be concentrated on this material. Initial results have been encouraging.

Integral coverslipped cells have been fabricated by high vacuum sputtering with up to 8 mils of SiO_2 . The quality of the SiO_2 is excellent. However, cells with thick coverslip layers exhibit serious curvature resulting from the stresses in the SiO_2 . The stress problem is under investigation.

The cell test results show every indication that when the deposition rate and stress problems have been solved, thick integral coverslips deposited by the techniques under development will satisfy all integral coverslipping technical requirements.

In some areas, the following report gives only a summation of results and conclusions. Detailed discussions may be found in previous Quarterly Reports.

INTRODUCTION

While development of thick solar cell integral coverslips proceeds directly from the accomplished development of thin integral coverslips, the path to the goal is technically difficult. Moreover, a variety of unexpected obstacles has been encountered. These technical problems, coupled with basic economic considerations, have forced some program modification.

The major point of integral coverslip development is to eliminate UV and radiation damage of the adhesive used to attach glued coverslips. A secondary aim is to give an improved cell power/weight ratio, through use of thinner (2 to 5 mil) coverslips, without increasing coverslip costs. (Thin glued slips are more expensive than thick glued slips.) A tertiary aim is to provide some measure of cell edge insulation and junction protection. These aims are guided by a firm realization that integral coverslips must not only be technically superior to glued slips, but must also be economically competitive. Prior to inception of this contract, IPC had attained these goals for 1 mil SiO_2 coverslips and was proceeding with equipment for production quantities. While this slip thickness is sufficient for many space missions, thicker slips are required for many others.

Several a priori technical limitations influence the development of integral coverslips. In the first place, no transparent inorganic material is a good thermal expansion match with silicon. This fact has two ramifications. Firstly, all high temperature deposition processes would be doomed to failure since either the cell would fracture or cell-slip bond would yield, on the post-deposition return, to room temperature. Secondly, since all deposition processes require some elevated temperature or equivalently energetic impingement of material, the cell-coverslip bond will be stressed. This suggests use of a deposition process that maximizes the strength of bond. Previous experience with IPC's proprietary high vacuum sputtering process suggested it was suited to this requirement. The second a priori limitation is that of the total of transparent inorganic materials, only fused silica and sapphire are known to be sufficiently radiation resistant to be acceptable. (Organic materials were not considered in this program to have all the necessary qualities for good coverslips.)

From the limitations noted above and the features of high vacuum sputtering, it appeared reasonable that this process should allow deposition of integral SiO_2 (or Al_2O_3) coverslips that satisfy environmental requirements. Such was found to be the case for coverslips up to 2 mils thick. Since this contract called for slips up to 20 mils thick, two paths could be followed. In the first place, high vacuum sputtering could be used to deposit the entire slip. In the second approach, a different deposition technique would be used to build-up slip thickness over an initial high vacuum sputtered slip. These twin approaches were initially based on economic considerations. The obtainable SiO_2 deposition rate from high vacuum sputtering is something under 10^4 Å/hr. While scaling

up high vacuum sputtering equipment to simultaneously slip a large number of cells is a straight-forward engineering task, increasing the deposition rate is technically difficult. Consequently, a large high vacuum sputtering system capable of simultaneously slipping several thousand cells to 3 mils is economically feasible, whereas devoting a machine to very long runs on thicker coverslips is not economically attractive. Thus, the two process path was favored.

A literature survey indicated that only reactive dc sputtering of Si (or Al) and electron beam evaporation of SiO_2 (or Al_2O_3) were useful as building up techniques. This choice was made on the basis of thermal processing limitations and deposition rate. It should be noted that the bond strength required between the two SiO_2 (or Al_2O_3) layers would not have to be as large as that required at the cell-slip interface since the only stress at the former interface would be due to stress inherent in the second stage deposition process itself. Thus, processes that are unacceptable for the initial layer could be used for building up thickness.

The unexpected element was the large stress inherent in the high vacuum sputtering process. At present, this stress appears to preclude deposition of all high vacuum sputtered slips thicker than approximately 6 mils. While a better understanding of the origin of this stress may allow a revision of these figures, it is likely that these stress levels are inherent to the high vacuum sputtering process. Thus, a two process thick coverslip would be desirable technically as well as economically.

Unfortunately, neither electron beam evaporation of SiO_2 nor dc reactive sputtering of Si at IPC has proved to be capable of giving optically acceptable thick layers of SiO_2 . Electron beam evaporation of SiO_2 has been thoroughly investigated at IPC and also with outside vendors. Of the over 300 samples run at IPC, no thick SiO_2 layers approaching optical quality were obtained. This appears to have been due to evaporation of devitrified SiO_2 . The presence of devitrified SiO_2 in the evaporation charge is caused by the extremely high viscosity of molten SiO_2 and, consequently, the need for a geometrically large charge. An expensive production electron beam evaporator that has been built by others might eliminate this problem, but indications are that the risk is a poor one in view of the high cost. Consequently, electron beam evaporation of SiO_2 has been abandoned.

On the other hand, electron beam evaporation of Al_2O_3 has been quite encouraging. Approximately 50 samples have been run with Al_2O_3 . The much lower viscosity of Al_2O_3 , as compared to SiO_2 , makes this evaporation much easier. Work on electron beam evaporation of Al_2O_3 will be continued. The prime advantage of electron beam evaporation is its high deposition rate.

Similarly, dc reactive sputtering of Si has not produced optically acceptable thick SiO_2 layers. While over 300 samples have been run in the various modifications of this system, all thick SiO_2 layers are optically

inhomogeneous. The inhomogeneity is a frothy white material not SiO_x . No evidence of SiO_x has been observed in properly prepared layers. The cause of the optical inhomogeneity is now thought to be known. It can only be eliminated by sputtering at much power pressures. However, this reduces the deposition rate to an unacceptable level. It is reported that dc + RF reactive sputtering in the 10^{-4} torr range gives deposition rates equivalent to those observed with dc reactive sputtering in the 10^{-2} torr range. Implementation of this approach is now in progress.

Since the other processes have not produced acceptable SiO_2 layers, all thick coverslips have been produced by high vacuum sputtering. While slips up to 8 mils thick have been produced, slips over 6 mils thick spontaneously fracture the cell at some time after slip deposition. Approximately 400 cells have been run by this process. In most cases, the slip thickness was continually increased until the cell fractured or the slip delaminated. During the early part of the contract, delamination was a major problem. This particular delamination problem has been essentially eliminated by improved pre-deposition cell cleaning techniques and improvements in the quality of the CeO_2 anti-reflective layer upon which the coverslip is deposited. Delamination of slips coated in certain regions of the high vacuum sputtering system has recently been observed. While this phenomenon is little understood at present, it appears to be associated with higher than normal stress in the cell and slip. In the case of thick slips, cracking of the cells during the run has often been observed. While this appears again to be a stress phenomenon, the slip thickness obtained before the cells cracked has followed a learning curve. Presently cells with 6 to 7 mil slips can be prepared without cracking during deposition. One 8 mil slip was prepared. It spontaneously cracked several weeks after preparation. It should be noted that thick slips which are not delaminated at the end of the deposition cycle do not delaminate on repeated rapid temperature cycling between 77 and 373°K. Moreover, thick slip cells that crack, either during or after deposition, are not delaminated. Refinement of the high vacuum sputtering process and investigations on the source of the inherent strain in the cells are being mainly supported by IPC, but are reported here. These investigations will continue.

Environmentally, the SiO_2 integral coverslipped cells have exhibited no measurable degradation under rapid temperature cycling between the previously noted temperature limits, prolonged exposure to UV radiation in hard vacuum at 100°C and exposure to 10^{15} protons-cm⁻² at 400 keV.

TABLE OF CONTENTS

<u>Section</u>		<u>Page</u>
	OBJECTIVE	iii
	FOREWORD	v
	SUMMARY	vii
	INTRODUCTION	ix
1	BENDING STRESS IN INTEGRAL COVERSIP CELLS	1
2	MATERIALS	9
3	DEPOSITION TECHNIQUES	11
	3.1 High Vacuum Sputtering	11
	3.2 Reactive Sputtering	16
	3.3 Electron Beam Evaporation	16
4	CELL TESTING	19
	4.1 Vacuum-UV Environment	19
	4.2 Proton Resistance	21
	4.2.1 Front Surface Irradiation	21
	4.2.2 Back Contact Irradiation	25
	4.3 Electron Irradiation	25
	4.4 Coverslip Results	25
5	FUTURE PLANS	35
6	REFERENCES	37

LIST OF ILLUSTRATIONS

<u>Figure</u>		<u>Page</u>
1	Stresses in an Integral Coverslip Cell	2
2	Cell Bow as a Function of High Vacuum Sputtered Integral SiO ₂ Coverslip Thickness	3
3	Radius of Curvature of High Vacuum Sputtered Integral SiO ₂ Coverslip Cell	4
4	Maximum Stress in SiO ₂ and in Si of Integral Coverslip Cells Produced by High Vacuum Sputtering	6
5	High Current High Vacuum Sputtering System Schematic	12
6	Production Coverslip Apparatus	13
7	Reactive Sputtering System	17
8	I-V Characteristics of (Solderless) Cell T3-80 Bombarded by 400 keV Protons on Back Surface	27
9	Reflected Intensity from CeO ₂ and SiO ₂ Anti-Reflective Coatings Optimized to 6000 Å with and without SiO ₂ Coverslip	29
10	I-V Characteristics of Cell A61-2B Before and After Coverslipping with 5 mil SiO ₂ Integral Coverslip	30
11	I-V Characteristics of Cell 623A-54A Before and After Coverslipping with 5 mil SiO ₂ Integral Coverslip	31
12	Absorption per mil of High Vacuum Sputtered SiO ₂ as a Function of Wavelength	33

LIST OF TABLES

<u>Table</u>		<u>Page</u>
1	Vacuum-UV Storage No. 2 Results	20
2	Vacuum UV Storage No. 3	22
3	Front Surface Proton Irradiation Test No. 1	23
4	Front Surface Proton Irradiation Test No. 2	24
5	Back Cell Contact Proton Irradiation	26

SECTION 1

BENDING STRESS IN INTEGRAL COVERSLIP CELLS

Growth of a layer of any material onto another material having different mechanical characteristics generally results in inherent stress of the deposited layer. Such stress is present to varying degrees in integral coverslips deposited by all available techniques. Curvature of the cell as a result of coverslip stress presents the most serious problem still to be overcome in the development of practical, thick integral coverslip cells. Thick, highly stressed coverslips result in serious bending which can complicate mounting and may fracture the cell.

As slip thickness increases, the coverslipped area of the cell becomes curved into a segment of a spherical surface. Developmental work has been done with 1 x 2 cm cells which, for the purpose of estimating stresses in the silicon and coverslip, will be considered to bend along their 2 cm dimension only. Neglecting curvature along the shorter dimension allows the problem to be treated as bending of a simple beam.

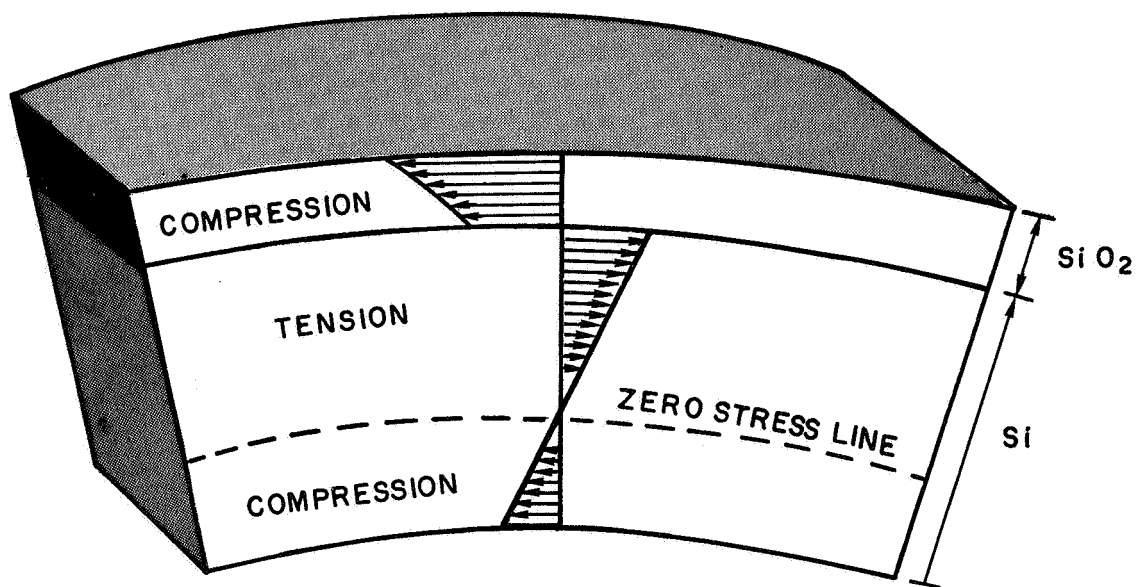
During coverslipping, cells are free to bend continuously as the slip thickness increases. The coverslip material is deposited at maximum stress but this stress becomes partially relieved as deposition continues and cell curvature increases. Consequently, stress in the coverslip varies smoothly from a maximum at the outer surface to a minimum at the cell-coverslip interface. Figure 1 shows the stresses that exist in a cell allowed to bend continuously as a stressed coverslip material is applied. Maximum stress in the Si is seen to be near the SiO₂-Si interface.

Figure 2 is a plot of cell bow as a function of slip thickness for a series of high vacuum sputtered SiO₂ coverslipped cells. Bow in this case was measured, as shown in the figure insert, by clamping one end of the cell and measuring the deflection of the other end. Simple geometric considerations can be used to show that from this measurement the radius of curvature, r , is well approximated by:

$$r = \frac{l^2}{2Z} \quad (1)$$

where l is the length of the cell (2 cm) and Z is the measured bow. The radius of curvature calculated using the experimental data of Figure 2 is shown in Figure 3 as a function of coverslip thickness.

The requirement that the cell be in static equilibrium allows film stress to be calculated as a function of measured curvature. Development of a rigorous analysis to include the effects of thick coatings, partial stress relief



Stress Magnitude Represented by Arrow Length

Figure 1 Stresses in an Integral Coverslip Cell

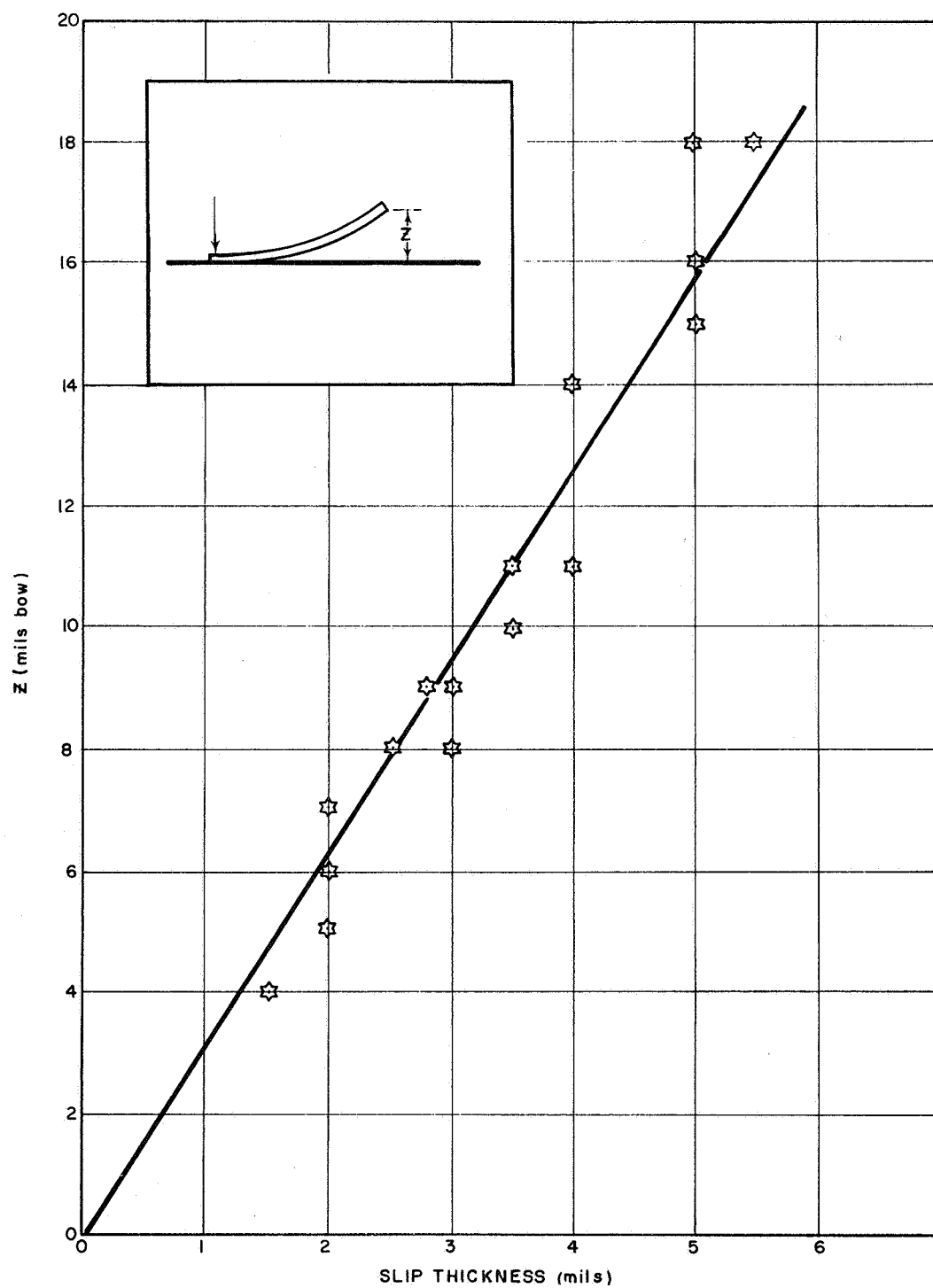


Figure 2. Cell Bow as a Function of High Vacuum Sputtered Integral SiO₂ Coverslip Thickness (1 x 2 cm 15 mil Thick Cells)

1-2461

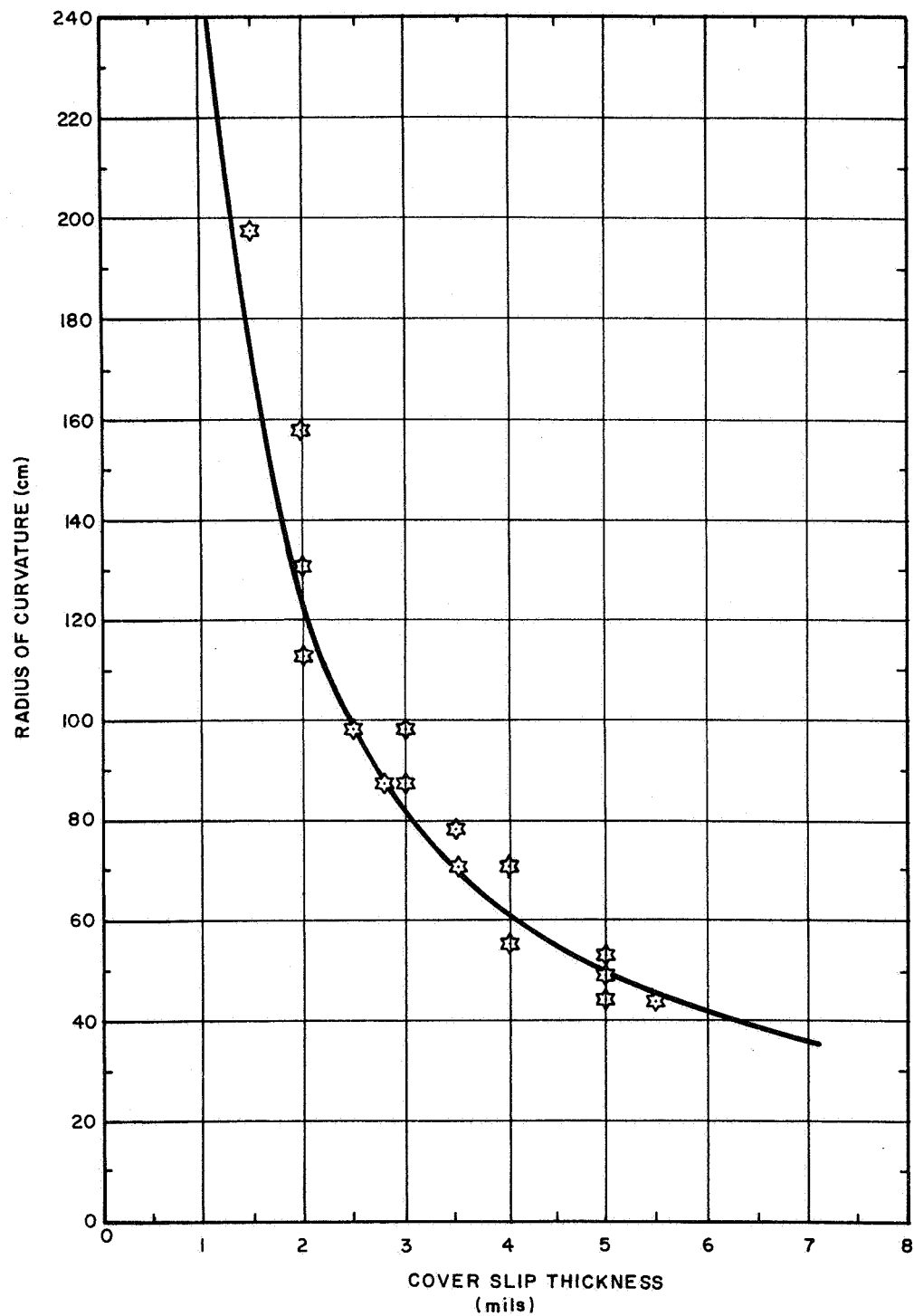


Figure 3. Radius of Curvature of High Vacuum Sputtered Integral SiO₂ Coverslip Cells (1 x 2 cm 15 mil Cells)

1-2462

through bending, and different Young's modulus of cell and coverslip is complex but has been carried out by Brenner and Senderoff.⁽¹⁾ For the case where the substrate is free to bend as the coating is applied, the maximum stress at the outer surface of the coating is approximately given by:

$$S_{\max(\text{coating})} = \frac{E_s t \left(t + \frac{E_c}{E_s} d \right)}{6 r d} \quad (2)$$

where:

$S_{\max(\text{coating})}$	= maximum stress in coating
E_s	= Young's modulus of substrate
t	= substrate thickness
E_c	= Young's modulus of coating
d	= coating thickness
r	= radius of curvature of coated substrate

It can be shown that in the substrate the zero stress line lies approximately two-thirds of the substrate thickness from the cell-coating interface. Then the maximum stress, $S_{\max(\text{substrate})}$, in the substrate is approximately:

$$S_{\max(\text{substrate})} = \frac{2}{3} \frac{E_s t}{r} \quad (3)$$

For silicon solar cells fabricated from (111) silicon, Young's modulus in the (111) plane is:⁽²⁾

$$E_{\text{Si}(111)} = 1.24 \times 10^{12} \text{ dynes/cm}^2$$

If the value of Young's modulus for the SiO_2 high vacuum sputtered coverslip is taken to be $10.4 \times 10^{11} \text{ dynes/cm}^2$, then Equations (2) and (3) can be used to estimate the maximum stress in both the Si and SiO_2 . The results are shown in Figure 4. The straight lines shown in this figure are the calculated maximum stresses corresponding to the straight line drawn through the original data of Figure 2. Contrary to expectation, the maximum stress in the SiO_2 apparently increases with slip thickness. Maximum stress in the coverslip occurs at the outer surface and is thought to be determined entirely by the characteristics of the deposition process. Because coverslip stress is partially relieved through bending, constant outer surface stress infers that cell bow should increase less than linearly with slip thickness. The fact that the experimental data indicate a linear increase may be attributed to an unexplained mechanism

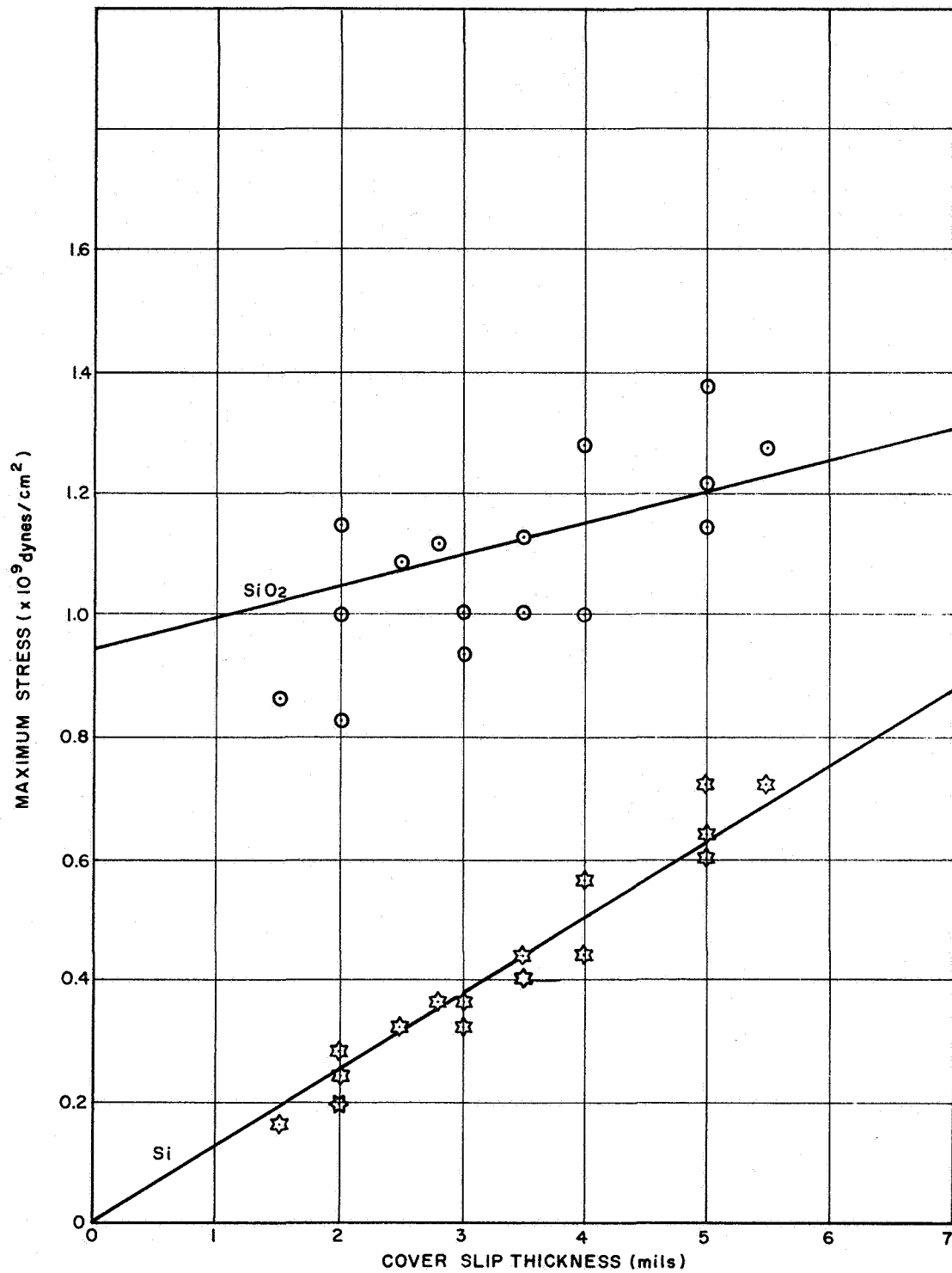


Figure 4. Maximum Stress in SiO₂ and in Si of Integral Coverslip Cells Produced by High Vacuum Sputtering

1-2463

or to the limited amount of thick slip data available and to measurement uncertainty. As more thick slip results are obtained, this conclusion will be re-examined.

The maximum stress in the coverslip is far below the ultimate compressive strength of SiO_2 , so that there is no problem of catastrophic collapse of the SiO_2 . However, it is seen that application of a 7 mil integral SiO_2 coverslip produces maximum stress in the silicon substrate equal to approximately 25% of the single crystal silicon mechanical fracture threshold of 3.5×10^9 dynes/cm².⁽³⁾ The presence of such high tensile stress appreciably increases the susceptibility of the cell to catastrophic failure.

SECTION 2

MATERIALS

The first requirement on candidate coverslip materials is that they be almost totally transmitting in the range 0.4 to 1.1 microns over which the solar cell is capable of useful energy conversion, and also that they remain almost completely non-absorbing in this band after ultraviolet, electron and proton exposure. Available, physically acceptable, stable materials which meet this requirement are fused silica (SiO_2), Al_2O_3 , Si_3N_4 , MgO and lead glasses. Initial experimental work with several lead glasses indicated that their thermal expansion characteristics are incompatible with those of silicon to the extent that they cannot be considered feasible integral coverslip materials.

Of the four remaining materials, the properties of the first two, SiO_2 and Al_2O_3 are best known and appear most compatible with the requirements of an integral coverslip cell. Consequently, experimental effort to date has involved only these, with emphasis concentrated on SiO_2 .

SECTION 3

DEPOSITION TECHNIQUES

3.1 High Vacuum Sputtering

The proprietary IPC high vacuum sputtering process utilizes a focused ion beam propagating through a high vacuum region to sputter the target material. At operating pressures below 10^{-4} torr, mean free path of the sputtered molecules is far greater than the target to substrate distance which insures that the sputtered molecules reach the substrate without collision and at maximum energy, thereby resulting in substrate surface penetration and excellent bonding. As the thermal expansion coefficients of all possible coverslip materials are considerably different from that of silicon, excellent bond characteristics are required in order that the cell will be able to survive thermal cycling without coverslip delamination.

Figure 5 is a schematic diagram of a typical IPC high vacuum sputtering system. Several such machines are presently being used for coverslip development work. Use of high vacuum sputtering results in the deposition of excellent quality, high purity, well bonded coatings onto the substrate. However, this process is rate limited which makes its use for the entire application of thick coatings economically undesirable if other more rapid techniques can be developed to build up acceptable quality material onto a well-bonded underlayer. At the present time, in the absence of such techniques for rapid build-up, development of thick coverslips must utilize long-term deposition in the high vacuum sputtering machines.

Deposition rate in the high vacuum sputtering machines is typically about 6000 \AA/hr^{-1} of SiO_2 . Therefore, application of thick slips requires approximately 65 hours per mil of SiO_2 . Deposition rate can be increased linearly with beam current density but only with increased system complexity. However, it is comparatively easy to maintain similar beam current density (and deposition rate) but increase deposition area in order that larger numbers of cells may be coated simultaneously. An IPC production sputtering machine, shown in Figure 6, has been designed to accommodate several thousand cells per run.

Integral SiO_2 coverslips up to 8 mils thick have been fabricated by high vacuum sputtering onto $1 \times 2 \text{ cm}$, 15 mil thick cells. However, as discussed in Section 1 of this report, cells with high vacuum sputtered SiO_2 coverslips of such thickness are curved and highly stressed. The radius of curvature of the one 8 mil coverslip cell produced was approximately 27 cm which made it difficult to mount properly for electrical testing. The stresses in the 4 to 8 mil coverslip cells fabricated were so large that the cells were fragile and fractured under relatively mild shock. Some of these cells, the single 8 mil coverslip cell for instance, survived normal handling for several weeks

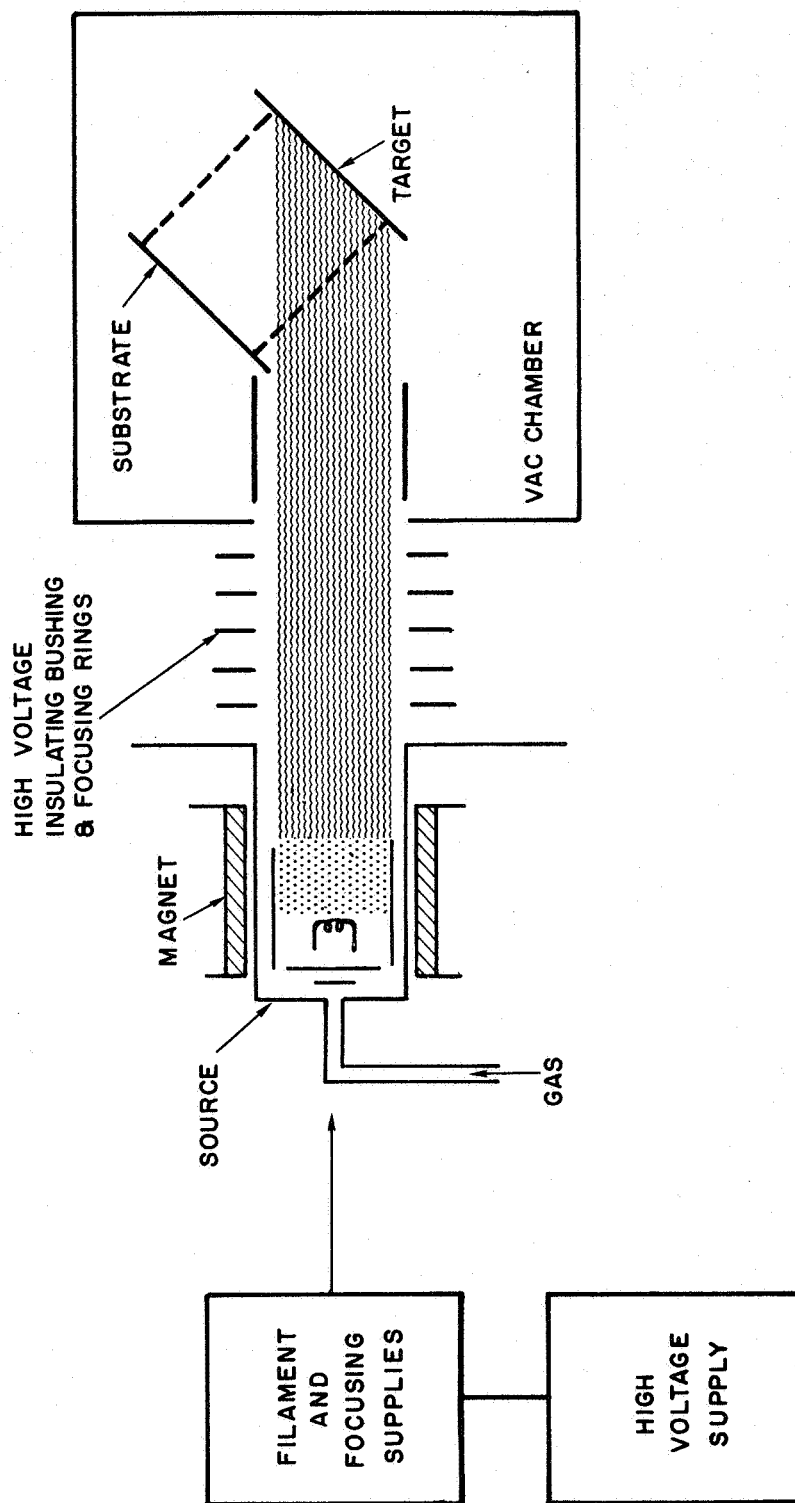


Figure 5. High Current High Vacuum Sputtering System Schematic

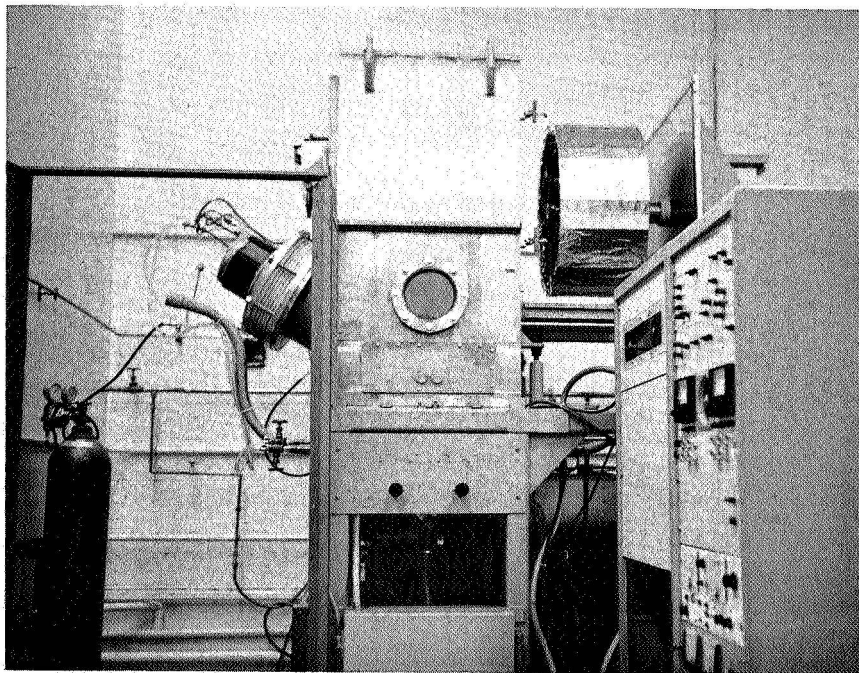


Figure 6 Production Coverslip Apparatus

and then spontaneously fractured while in storage. When a cell fractures, although it seems likely that failure of the silicon occurs first, the cell and coverslip fracture together to give a number of individual fragments, each still bonded at the cell-coverslip interface.

During the early period of this development program, delamination of the coverslip during and shortly after application was a serious problem. In addition to this, it was found that temperature cycling resulted in the onset of peeling of the coverslip at cell corners. The cause of delamination was traced to a combination of inadequate cell cleaning prior to sputtering, unsatisfactory quality CeO_2 in the anti-reflective coating and to contamination of the sputtering beam through contact with the chamber orifice and mechanical components. Improved cleaning techniques utilizing a high pressure spray of hot solvent have eliminated bond failure resulting from traces of impurities trapped between the cell and coverslip. Minor changes and introduction of rigid quality control in the evaporation procedure for application of the CeO_2 led to anti-reflective films which are sufficiently well bonded to the silicon to prevent delamination. Solution of the last of the noted delamination problems was attained by modification of the sputtering apparatus to improve beam control and insure that none of the beam strikes the chamber.

The low deposition rate of high vacuum sputtering without an adequate alternative high rate process makes production fabrication of SiO_2 integral coverslips time consuming, if thick coverslips are required. The cell curvature resulting from the application of thick integral coverslips requires special handling and mounting techniques. Significant reduction of the stress problem causing the curvature must be accomplished before cells with thick integral coverslips could gain widespread acceptance. For this purpose, two approaches are being pursued:

- (1) determination of the mechanism responsible for the stress and development of appropriate correction,
- (2) development of techniques which result in the deposition of unstressed or only moderately stressed coverslip material.

The former approach involves a careful study of the effects of charges in sputtering conditions on cell stress levels while the latter study involves investigation of building-up techniques other than high vacuum sputtering and/or materials other than SiO_2 .

Cell curvature as a result of coverslipping has been analyzed in detail in Section 1. Similar curvature and stress occur in SiO_2 coatings grown at high temperature. In this case, the stress is due to thermal expansion mismatch (cell curvature has also been reported in deposition of RF sputtered SiO_2 coverslips). Since curved samples are obtained when high vacuum sputtered

SiO_2 is deposited onto thin SiO_2 coverslides, the observed cell curvature is not associated with thermal expansion coefficient mismatch. Curvature in the case of high vacuum sputtering is due to an inherent film stress that increases with film thickness. This stress could arise from several causes. Firstly, it may be due to limited surface mobility of the incident SiO_2 on the growth face. If this were the case, elevated substrate temperatures should increase surface mobility and thus lower cell curvature. Coverslip deposition at substrate temperatures of 27°C, 120°C, 230°C and 400°C all, however, resulted in similar cell curvature. This indicates that either limited surface mobility is not the main problem or, and more likely, practical substrate temperatures are insufficient to produce the necessary surface mobility. A more probable source of the film stress is that high vacuum sputtering proceeds through the deposition of highly energetic molecules. The considerable kinetic energy (up to 100 eV) of these molecules allows them to penetrate the growth face into previously deposited material. This penetration would result in gradual expansion of the deposited layer near the surface and consequently increased stress and cell curvature. This mechanism is obviously a case of essentially zero surface mobility.

Annealing of coverslipped cells at temperatures up to 450°C produced no measurable change in their curvature. As the coefficient of thermal expansion of Si is greater than that of SiO_2 , it is expected that at elevated temperatures, cell curvature should be reduced. This was checked by heating several cells on a hot plate while their curvature was observed. At up to 500°C, there was no measurable change in cell curvature. In another experiment, a 2 mil thick SiO_2 slip was removed, partially intact, from a coverslipped cell by heating to 800°C in a Cl_2 atmosphere. Where radius of curvature of the complete cell had been approximately 70 cm, the radius of the free SiO_2 slip was roughly 5 cm. These results suggest that energetic sputtered material does, indeed, penetrate the growth face into the previously deposited material, thereby forcing the surface of the sputtered coating to expand. The other surface then becomes increasingly longer as slip thickness increases. It should, however, be noted that this penetration produces the tight SiO_2 -Si bonding that is required for coverslip retention during thermal cycling.

Investigations to determine means of reducing stress associated with high vacuum sputtering of thick SiO_2 will be continued, since it is the only technique that has been shown to be capable of producing the bond strength required for satisfactory bonding of thick coverslips. Once a strong bond has been formed between the coverslip material and the cell, however, the same material deposited by another less adherent but more rapid process may then be used to build up the thickness as the conditions on bond strength required of this process are less stringent.

3.2 Reactive Sputtering

Good, thick reactively sputtered films of SiO_2 have not yet been made. Thick films suffer from physical and optical inhomogeneity, the cause of which is thought to be known. SiO_2 deposition rates of $25 \times 10^3 \text{ \AA hr}^{-1}$ have been observed.

Many modifications of the reactive sputtering apparatus have been made in the effort to improve film quality. Stage-by-stage modifications and their effects are detailed in earlier reports. The present arrangement of the system is shown in Figure 7. Although reactively sputtered SiO_2 is now superior in quality to that produced earlier in the program, it still exhibits inhomogeneity to a degree that it cannot yet be considered acceptable for the building up process.

As it now stands, the major problem seems likely to be explained by analogy to the work of Janus and Shirn⁽⁵⁾ as backscattering of sputtered SiO_2 onto the silicon cathode. When thin SiO_2 films are sputtered, the quantity of SiO_2 backscattered onto the cathode is very small and does not interfere with sputtering. However, as the SiO_2 builds up, the cathode may become patchy and at some point breakdown will then occur through these dielectric islands. This might directly dislodge macroscopic particles of the backscattered SiO_2 which would then float to the substrate to be overcoated or, because of the energy density in the discharge, devitrification of the SiO_2 islands might also occur along with detachment. Backscattering can be decreased by reduction of the pressure but unfortunately decreased deposition rate would also result. As RF and RF plus dc reactive sputtering processes yield high deposition rates at lower gas pressures, they will be employed in future work.

3.3 Electron Beam Evaporation

Work on electron beam evaporation of SiO_2 has been dropped because of poor results. All thick SiO_2 deposited by electron beam evaporation has been both highly stressed and physically inhomogeneous. The deposited material was invariably relatively soft, had low refractive index and contained a high density of second phase optical scattering centers. These inhomogeneities are thought to be associated with evaporation of devitrified SiO_2 . Film quality could not be significantly improved through variation of the evaporation conditions. Thick evaporated SiO_2 supplied by several outside vendors was of similar unacceptable quality. Although equipment could possibly be designed to produce good thick evaporated SiO_2 , construction costs would be prohibitive and consequently it has been decided to discontinue work on SiO_2 in favor of a more attractive alternate, Al_2O_3 .

A major difficulty in the electron beam evaporation of SiO_2 is that the molten silica does not flow but instead craters in the beam, thereby making

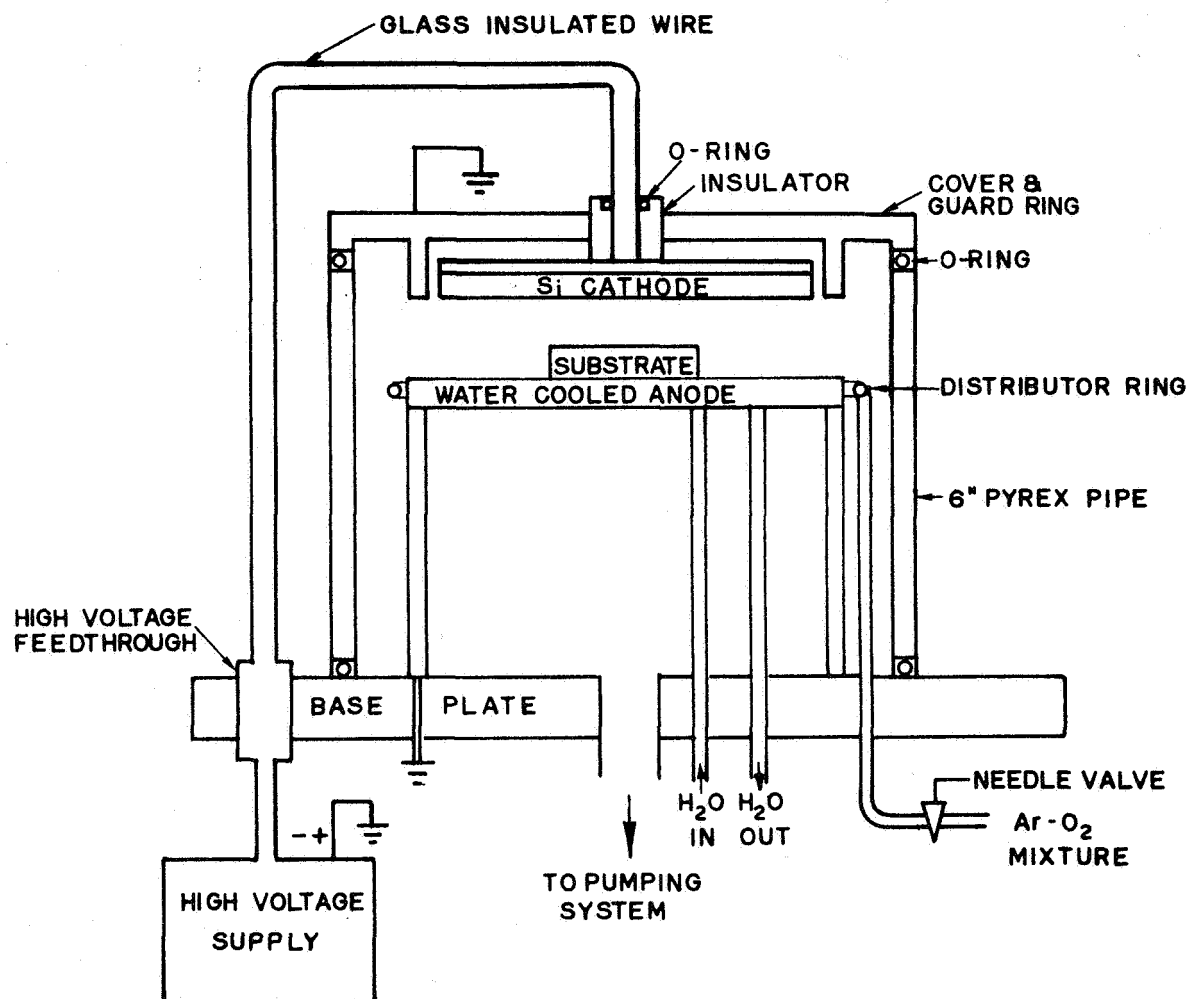


Figure 7. Reactive Sputtering System

it difficult to maintain a broad evaporating surface. The viscosity of molten Al_2O_3 is, on the other hand, sufficiently low for flowing to occur and a good surface is maintained. Electron beam evaporation of Al_2O_3 has been quite successful. While quoted deposition rates are approximately one-fifth those of SiO_2 , rates of $300 \times 10^3 \text{ \AA hr}^{-1}$ should be obtainable from a 2 kw gun with 10 inch gun-substrate spacing. (Because Al_2O_3 is almost twice as dense as SiO_2 , only half the Al_2O_3 thickness is required.) A limited number of runs have been made in which good quality thick Al_2O_3 has been evaporated over a thin layer of high vacuum sputtered Al_2O_3 . Adherent films up to 2 mils thick have been deposited. Substrate cleaning appears to be more critical for evaporated Al_2O_3 than it was for evaporated SiO_2 . With properly cleaned substrates, 2 mil Al_2O_3 films can be temperature cycled from -196°C to $+100^\circ\text{C}$ without delamination. The evaporated Al_2O_3 does not appear to be as highly stressed as evaporated SiO_2 . This work will be continued.

SECTION 4

CELL TESTING

4.1 Vacuum-UV Environment

Test 1

Two integral coverslip cells were stored for 500 hours at $100 \pm 1^\circ\text{C}$ in a vacuum of 2 to 8×10^{-7} torr. No weight loss or physical deterioration of the cells was observed.

Test 2

With UV irradiation capability added to the vacuum environment apparatus, six 1 x 2 cm cells, three regular and three with 1 mil SiO_2 integral coverslips were subjected to 509 hours exposure to the UA-2 mercury vapor lamp at approximately 20 mw/cm^2 . Cell temperature was $130 \pm 2^\circ\text{C}$ and pressure was 2 to 8×10^{-7} torr.

In this run, the mercury vapor lamp was installed inside the vacuum chamber. Continuous operation of the lamp in vacuum resulted in evaporation of cement from the lamp ends. This contaminant was deposited in the form of a thin film over the cells and throughout the entire vacuum chamber. Because of the presence of the film, the test was interrupted after 156 hours and the cells were tested before resumption of the irradiation. The data are tabulated in Table 1.

The changes in the uncoverslipped cells lie within the measurement uncertainty and could be partially due to the contaminating film. The changes in coverslip cells 53-19 and 53-37 are real, but are attributed to the fact that these cells were made early in the program when delamination was yet an unsolved problem. The coverslips of these cells had delaminated at the corners during the UV irradiation. Delamination results in light loss through scattering. The changes in output characteristics of cell A61-12A which did not begin delaminating are equivalent to those of the uncoverslipped cells.

Test 3

To eliminate the problem of contamination of the cells and vacuum system by evaporated material from the UV lamp, the light source was remounted outside the chamber and a 6 inch diameter by 0.5 inch thick Dynasil fused silica window was used to transmit the UV onto the cells. The window transmission is greater than 90% down to 2800 \AA and falls to 50% at approximately 2100 \AA . System geometry was such that intensity at the test cell location was approximately 20 mw/cm^2 as in the previous test.

Table 1. Vacuum-UV Storage No. 2 Results

Cell	Type	Hours of Irradiation	I_{sc} (ma)	V_{oc} (V)	I_{mp} (ma)	V_{mp} (V)	Curve Factor	Tungsten Efficiency (%)
623B-1	Regular	Initial	77	0.555	71	0.46	0.765	13.0
		156	76	0.555	70	0.46	0.765	12.8
		509	77	0.555	71	0.455	0.755	12.8
623B-4	Regular	Initial	81	0.555	74	0.46	0.76	13.5
		156	79	0.56	73	0.46	0.76	13.3
		509	80	0.555	75	0.45	0.76	13.4
623B-11	Regular	Initial	81	0.56	75	0.455	0.75	13.5
		156	81	0.555	74	0.45	0.74	13.2
		509	81	0.555	74	0.45	0.74	13.2
53-19	Coverslip	Initial	82	0.56	74	0.45	0.725	13.2
		156	78	0.56	70	0.45	0.72	12.5
		509	78	0.555	70	0.45	0.73	12.5*
53-37	Coverslip	Initial	84	0.56	77	0.455	0.745	13.9
		156	79	0.555	72	0.455	0.75	13.0*
		509	81	0.555	74	0.445	0.735	13.1*
A61-12A	Coverslip	Initial	82	0.555	74	0.45	0.73	13.2
		156	80	0.56	74	0.46	0.76	13.5
		509	78	0.56	72.5	0.45	0.75	13.0

* Coverslip beginning to lift noticeably

Average Efficiency Change

Cell Type	Exposure	Percent of Initial Efficiency Remaining
Regular	156 hr	98.2
	509 hr	98.5
Coverslip	156 hr	96.8
	509 hr	95.8

Three unslipped cells and three 1 mil SiO_2 integral coverslip cells (all 1 x 2 cm x 15 mil thick n/p cells with 7 finger contacts) were tested for 500 hours. The data is summarized in Table 2. One of the coverslip cells was accidentally broken during removal from the chamber after 500 hours. The other two coverslip cells confirm that UV degradation of sputtered integral coverslip cells is well within measurement error.

4.2 Proton Resistance

4.2.1 Front Surface Irradiation

All cells tested were 1 x 2 cm 15 mil thick n/p cells with 1 to 2 mil integral SiO_2 coverslips.

Test 1

Two cells were irradiated to 10^{15} protons/cm² by 400 keV protons. Contact bar metallization was of insufficient thickness ($\sim 10^4$ Å) to prevent radiation damage in the silicon immediately below the contact bar. Consequently, the cells exhibited reduced V_{OC} and curve factors. Annealing in argon at 400°C for 1 hour restored pre-irradiation output characteristics. Results are given in Table 3.

Test 2

Four cells were successively irradiated to 10^{13} , 10^{14} and 10^{15} protons/cm² at 400 keV with a metal mask covering the unslipped contact bar. The results of this test are tabulated in Table 4.

The listed values of AMO solar efficiency are based on conversion of relative spectral response data to an absolute efficiency by means of a computer program. Overall accuracy of testing procedures is estimated to be approximately $\pm 3\%$.

The coverslips on all the cells of this test were at least 1 mil thick which is more than adequate to stop 400 keV protons. Cells G4-45 and G5-17 had been irradiated in the previous proton test and subsequently annealed at 400°C for 1 hour to restore their initial characteristics. A small fault developed in the coverslip of G5-17 during the annealing and became noticeably larger during irradiation. The degradation in performance of G5-17 is attributed to the growth of this bubble. Cells G4-44 and G4-45 had two small ($\sim 1 \times 2$ mm) notches etched through the coverslip on the 2 cm edge opposite the contact bar.

The results demonstrate that integral coverslip cells with properly protected contact bars can withstand, without significant degradation, exposure to a high flux of protons of energy insufficient to penetrate the coverslip.

Table 6. Vacuum UV Storage No. 3*

		I_{sc} (ma)	V_{oc}	I_{mp}	V_{mp}	CF	Tungsten Efficiency
Bare	T3-1	initial	0.55	76	0.44	0.71	13.3%
		500 hr	0.55	73	0.44	0.71	12.7%
	T3-2	initial	0.56	75+	0.45	0.73	13.4%
		500 hr	0.56	74	0.45	0.73	13.2%
	T3-3	initial	0.545	72	0.44	0.73	12.6%
		500 hr	0.555	73	0.44	0.72	12.7%
Coverslip	61-1	initial	0.56	75	0.45	0.74	13.4%
		500 hr	0.56	75	0.45	0.74	13.4%
	61-18A	initial	0.55	75	0.44	0.74	13.1%
		500 hr	0.55	72	0.44	0.73	12.6%
	56-32	initial	0.55	71	0.44	0.70	12.4%
	**	500 hr	--	--	--	--	--

* 1 x 2 cm x 15 mil thick n/p (10 ohm-cm) cells with standard 7 finger contact

** Broken after storage but before reading

Table 7. Front Surface Proton Irradiation Test No. 1

Cell	Condition	I _{sc}	V _{oc}	Curve Factor
G4-45	Initial	80 ma	0.555 V	0.76
	10 ¹⁵ p/cm ²	80	0.53	0.72
	After Anneal	79	0.555	0.75
G5-17	Initial	82 ma	0.55 V	0.74
	10 ¹⁵ p/cm ²	80	0.537	0.695
	After Anneal	82	0.55	0.72

Table 8. Front Surface Proton Irradiation Test No. 2

Cell	Test	Proton Flux (p/cm ²)			
		0	10 ¹³	10 ¹⁴	10 ¹⁵
G4-45	I _{sc} (ma)	81	81	81	80
	V _{oc} (V)	0.555	0.555	0.555	0.555
	Curve Factor	0.76	0.75	0.75	0.76
	AMO Efficiency (%)	9.9	10.0	10.1	10.1
	Tungsten Efficiency (%)	13.6	13.4	13.4	13.4
G5-17*	I _{sc} (ma)	82	82	82	81
	V _{oc} (V)	0.555	0.555	0.555	0.555
	Curve Factor	0.75	0.685	0.70	0.715
	AMO Efficiency (%)	10.1	9.1	9.5	9.7
	Tungsten Efficiency (%)	13.5	12.3	12.6	12.7
G4-44	I _{sc} (ma)	82	82	82	81
	V _{oc} (V)	0.565	0.565	0.565	0.565
	Curve Factor	0.755	0.735	0.735	0.74
	AMO Efficiency (%)	10.5	10.1	10.4	10.4
	Tungsten Efficiency (%)	14.0	13.5	13.5	13.5
G5-8B	I _{sc} (ma)	80	81	81	81
	V _{oc} (V)	0.56	0.565	0.56	0.56
	Curve Factor	0.73	0.71	0.71	0.70
	AMO Efficiency (%)	10.1	9.7	10.1	10.0
	Tungsten Efficiency (%)	13.0	12.9	12.8	12.6

* This cell had a growing coverslip blemish.

4.2.2 Back Contact Irradiation

To determine the necessity of protecting the back surface of the solar cell as well as the front surface against damaging radiation, the rear contacts of solderless cells have been irradiated with 400 keV protons. The data from one such test is tabulated in Table 5 and I-V characteristics of a typical cell are shown in Figure 8.

Under the 400 keV proton bombardment, performance degradation begins at a fluence of approximately 10^{12} protons/cm². Efficiencies drop to 50% of initial values at approximately 1.5×10^{13} protons/cm². The degradation is thought to result from a radiation damaged high resistivity layer immediately beneath the back contact.

Cell mount assemblies utilizing solid backing behind the cells provide adequate protection against this type of radiation damage. However, open grid modules which leave the rear surfaces exposed would require additional protection. As indicated at the bottom of Table 5, exposure of the rear contact surface of a cell having a 1.3 mil integral SiO₂ coverslip over the rear contact to 10^{14} protons/cm² produced no reduction in cell efficiency. (A small portion of the surface left without coverslip in order to facilitate electrical contact was protected during the proton bombardment.) Similar irradiation of unprotected cells resulted in 90% degradation (see Figure 8).

4.3 Electron Irradiation

Shielding complications in the operation of the 2 MeV Van de Graaff generator prevented completion of electron resistance testing. Since the program funding was exhausted on other phases of the program, it was decided to forego electron testing until sometime in the contract extension. This is expected to have no noticeable effect on program performance since electron degradation should be only a bulk material effect, and therefore consistent with previous results obtained by many investigators.

4.4 Coverslip Results

Anti-reflective coatings for silicon solar cells are generally peaked at approximately 6000 Å in order to maximize the product of the solar spectrum and the photon response spectrum of the cell. At wavelengths other than that for which reflection is minimized, the anti-reflective coating spectral reflectance never exceeds the reflectance of the uncoated substrate. Total anti-reflection at a specific wavelength occurs when reflections from the upper and lower surfaces of the coating are equal in amplitude and opposite in phase. This requires that the coating thickness be an odd integral multiple of quarter wavelengths and that the refractive indices be related by:

Table 5. Back Cell Contact Proton Irradiation

Protons/cm ²	Cell*	I _{SC} (ma)	V _{OC} (volt)	I _{mp} (ma)	V _{mp} (volt)	Curve Factor	AMO Efficiency (%)
Initial	T3-78	64.1	0.557	56	0.450	0.71	9.5
	T3-79	65.0	0.561	60	0.456	0.75	10.3
	T3-80	64.2	0.555	59	0.453	0.75	10.1
	T3-81	65.5	0.556	59	0.454	0.74	10.1
	T3-82	68.0	0.560	62	0.440	0.72	10.3
10 ¹¹	T3-78	64.0	0.552	58	0.450	0.74	9.8
	T3-79	63.2	0.556	60	0.450	0.77	10.2
	T3-80	63.0	0.551	58	0.446	0.75	9.8
	T3-81	63.0	0.552	59	0.437	0.74	9.7
	T3-82	67.0	0.558	61	0.438	0.72	10.0
10 ¹²	T3-78	64.0	0.552	57	0.446	0.72	9.6
	T3-79	64.2	0.560	59	0.448	0.74	9.9
	T3-80	63.7	0.552	58	0.450	0.74	9.8
	T3-81	63.6	0.554	57	0.450	0.73	9.6
	T3-82	67.7	0.558	61	0.435	0.70	10.0
10 ¹³	T3-78	63.5	0.507	42	0.350	0.46	5.5
	T3-79	60.1	0.521	44	0.366	0.51	6.1
	T3-80	63.0	0.510	45	0.345	0.48	5.8
	T3-81	62.6	0.516	42	0.357	0.46	5.6
	T3-82	59.7	0.514	42	0.363	0.50	5.7
10 ¹⁴	T3-78	36.0	0.365	18	0.192	0.26	1.3
	T3-79	25.7	0.392	15	0.225	0.33	1.3
	T3-80	31.6	0.374	15	0.210	0.27	1.2
	T3-81	26.8	0.382	15	0.200	0.29	1.1
	T3-82	27.1	0.391	16	0.225	0.34	1.4
Initial 10 ¹⁴	cell with 1.3 mil quartz coverslip over rear con- tact	64.0	0.567	59	0.468	0.76	10.4
		62.0	0.574	58	0.476	0.78	10.4

* All cells 1 x 2 cm, anti-reflected, carbon arc AMO conditions

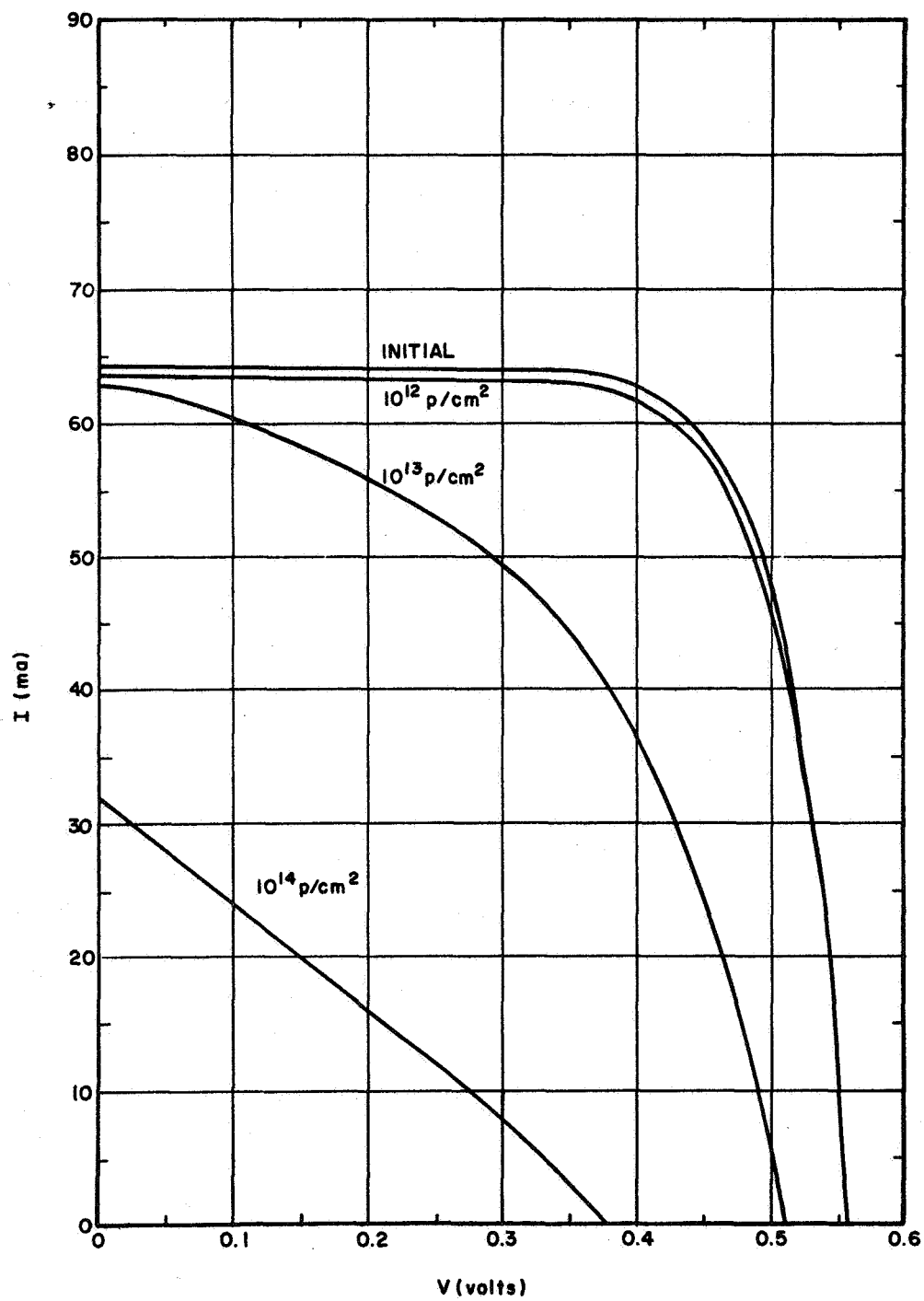


Figure 8. I-V Characteristics of (Solderless) Cell T3-80
Bombarded by 400 kev Protons on Back Surface

1-2215

$$n_{\text{layer}} = \sqrt{n_o n_{\text{Si}}}$$

where n_{layer} and n_{Si} are the refractive indices of the anti-reflective layer and silicon, respectively, and n_o is the index of free space in the case of a bare cell and of the coverslip material for an integral coverslip cell. In the case of the bare cell, assuming a refractive index of 4 for Si, optimum index of the coating should be:

$$n = \sqrt{n_{\text{space}} n_{\text{Si}}} = \sqrt{1.0 \times 4.0} = 2.0$$

and for an SiO_2 coverslip cell:

$$n = \sqrt{n_{\text{SiO}_2} n_{\text{Si}}} = \sqrt{1.46 \times 4.0} = 2.4$$

CeO_2 has refractive index 2.35 to make it an excellent material for use with coverslip cells but less suited for uncoverslipped cells. A cell with a CeO_2 anti-reflecting layer should exhibit an efficiency increase of approximately 1% after coverslipping. On the other hand, SiO, a commonly used anti-reflective coating material which has index 1.95 produces better anti-reflection characteristics on cells without coverslips, but shows a loss on application of a coverslip. Shown in Figure 9 is the fraction of incident intensity reflected as a function of wavelength from bare and coverslip cells using CeO_2 or SiO anti-reflective coatings optimized to 6000 Å. Included in the coverslip curves is the 3.5% loss from the SiO_2 surface. The refractive index of adhesive material is neglected. It can be seen that SiO is the better material on the bare cell and that CeO_2 is superior for the coverslip cell. The overall improvement through coverslipping in anti-reflection of a cell with CeO_2 coating is also apparent. MgF_2 may be used to reduce reflection at the SiO_2 surface.

In principle, a cell with a transparent integral coverslip and properly selected CeO_2 anti-reflective coating at the cell-coverslip interface exhibits greater absolute efficiency than the same cell in the absence of the coverslip. But, although anticipated, this result has so far generally not been observed in the development of sputtered integral coverslip cells. It is found that, as a result of the coverslipping operation, a few cells gain in efficiency, a few show significant efficiency loss and most remain approximately the same. Tungsten I-V characteristics before and after coverslipping of two cells with 5 mil integral SiO_2 slips are shown in Figures 10 and 11. Cell A61-2B showed only small tungsten efficiency loss from 13.3% before coverslipping to 12.9% after, while 623A-54A experienced anomalously large degradation from 13.6% to 11.2%.

A sample of 35 cells was tested before and after application of 2 mil integral coverslips. Average efficiency after coverslipping was found to be 99% of the initial average efficiency. Apparently during the coverslipping

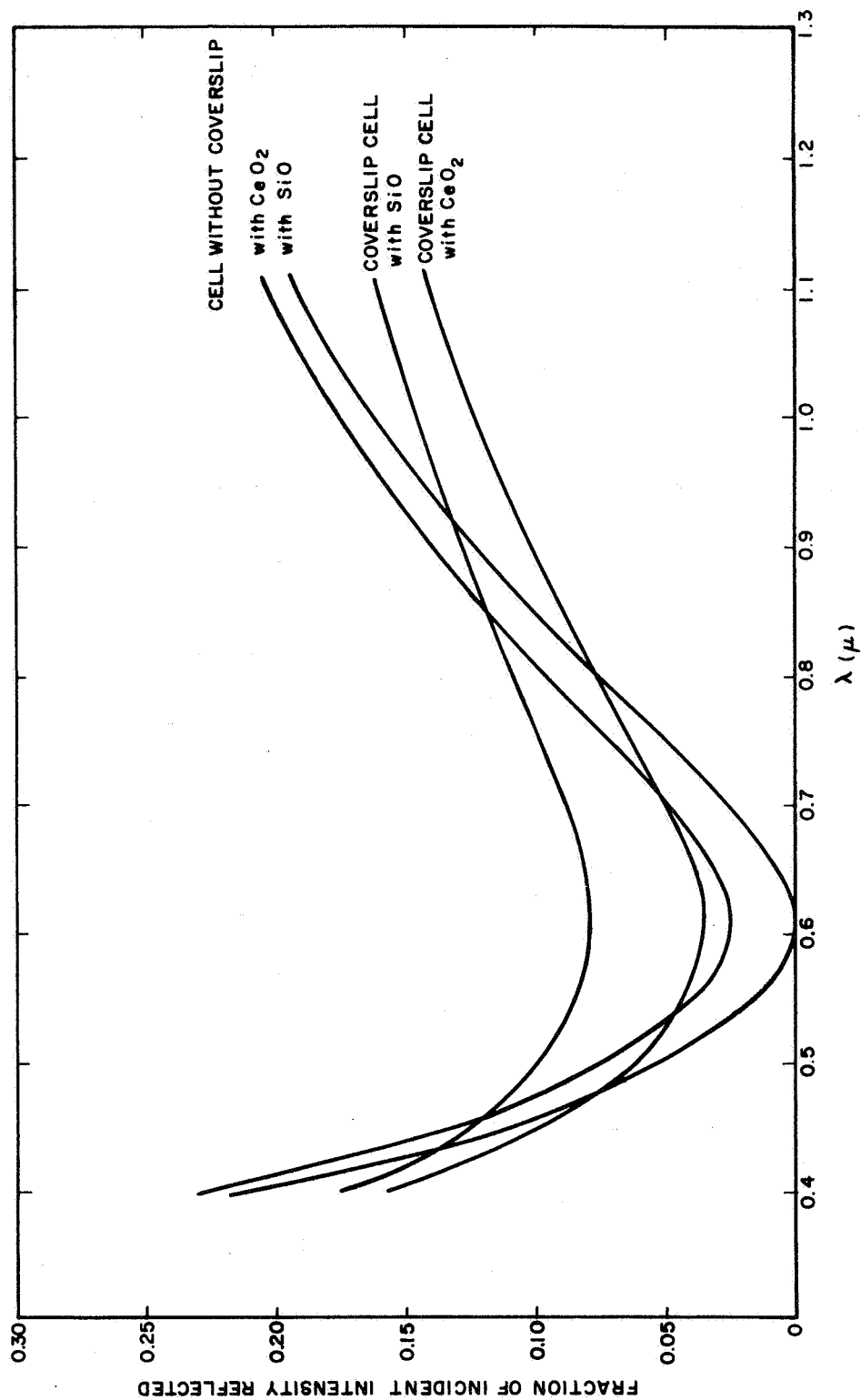


Figure 9. Reflected Intensity from CeO₂ and SiO Anti-Reflective Coatings Optimized to 6000 Å with and without SiO₂ Coverslip

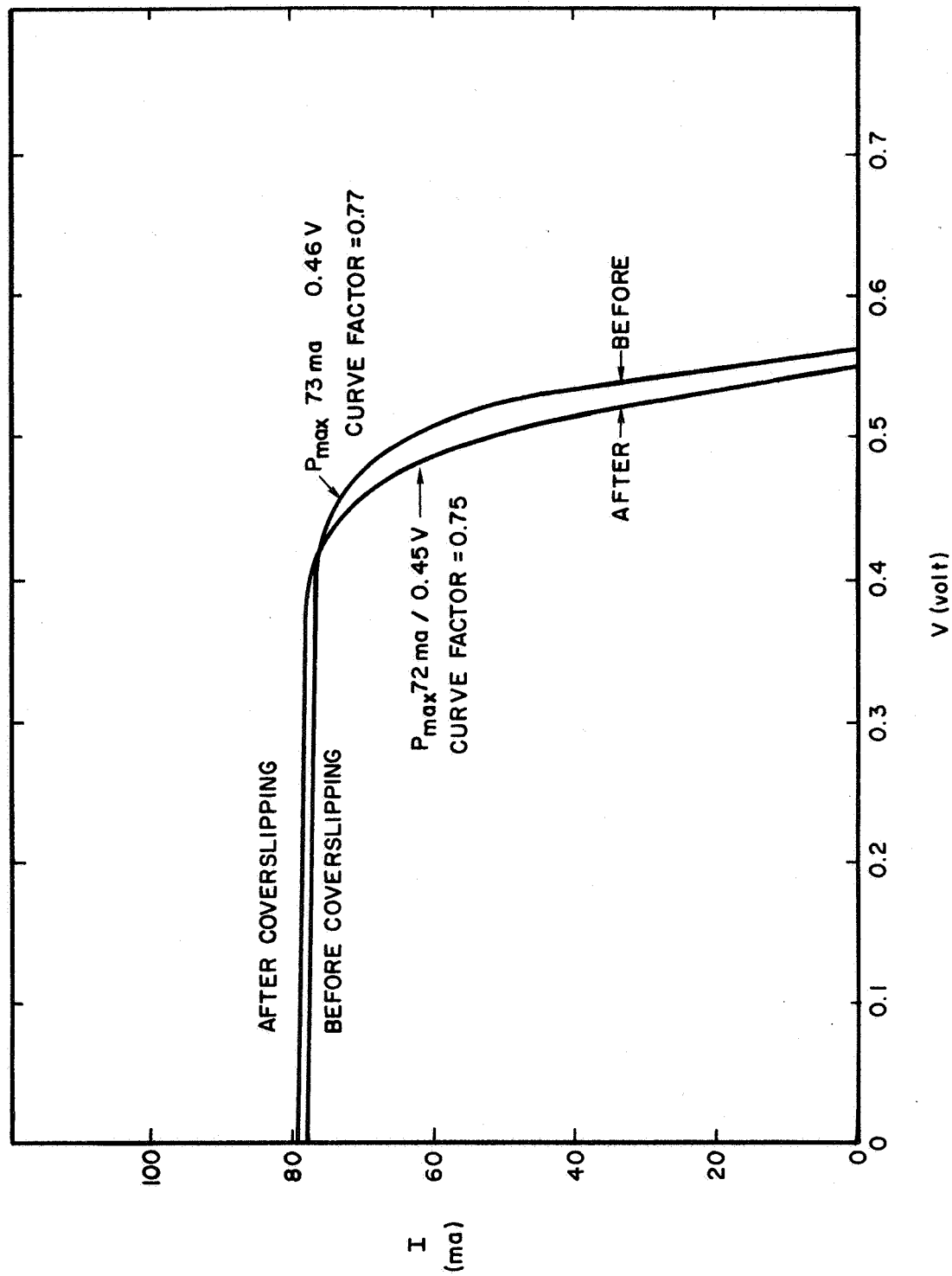


Figure 10. I-V Characteristics of Cell A61-2B Before and After Coverslipping with 5 mil SiO_2 Integral Coverslip

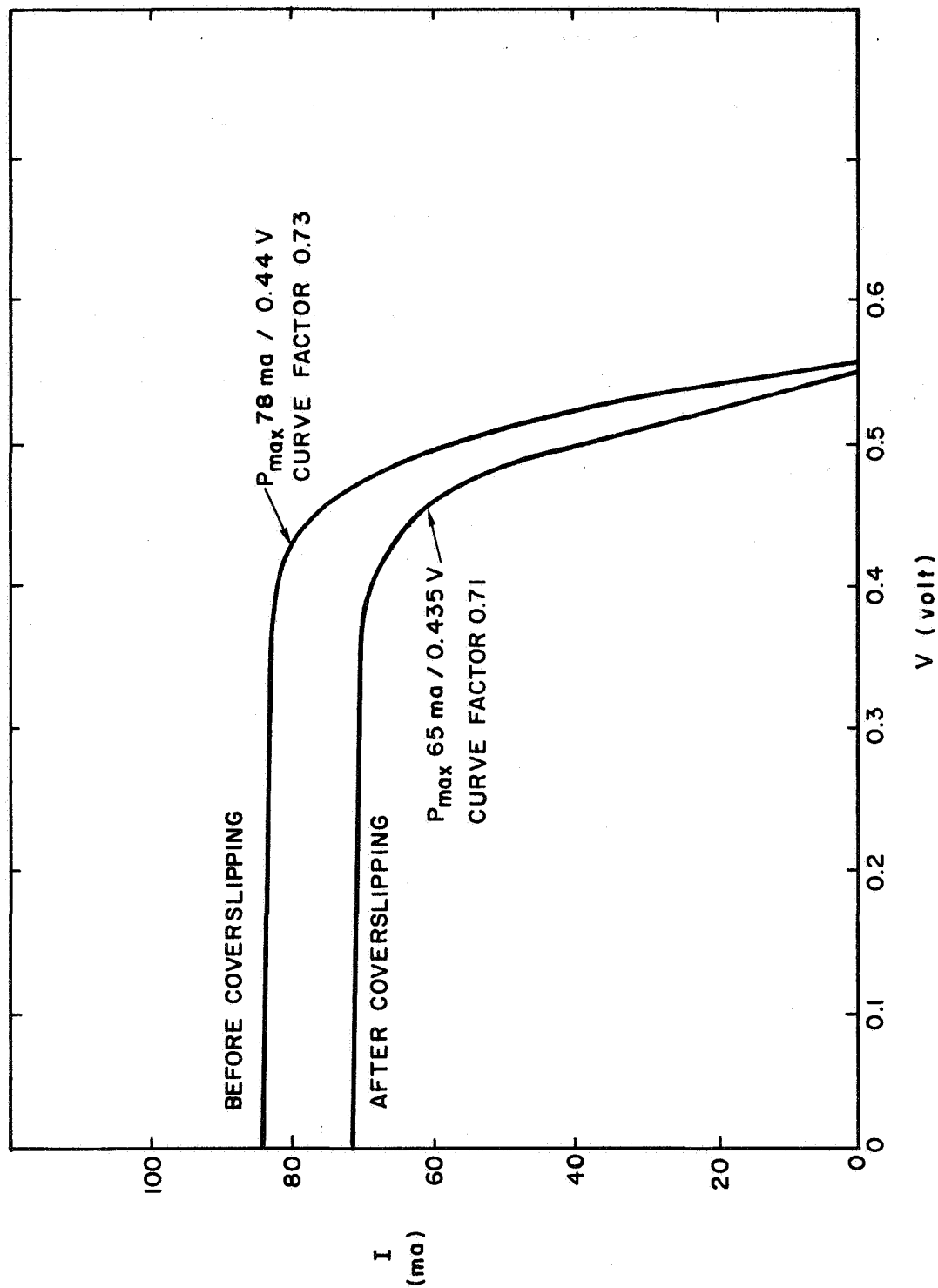


Figure 11. I-V Characteristics of Cell 623A-54A Before and After Coverslipping with 5 mil SiO_2 Integral Coverslip

operation, cell degradation occurs which is partially masked by the gain due to the presence of the coverslip. The most logical causes of the degradation are:

- (1) damage to the cell by sputtering,
- (2) light absorption in the coverslip,
- (3) light scattering from scattering centers in the coverslip.

Tests have indicated the sputtering damage loss to be approximately 1.5% of the initial efficiency. The mechanism for this damage is not understood as the 800 Å layer of CeO_2 used as anti-reflective coating should be sufficient to prevent penetration of the sputtered material to the silicon. Moreover, no observable change occurs in the CeO_2 layer thickness or refractive index. Transmission of high vacuum sputtered SiO_2 in the 0.4 to 1.1 micron wavelength band is sufficiently high that efficiency loss through absorption is less than 1% per mil of coverslip. A typical absorption curve for SiO_2 is plotted in Figure 12. Efficiency loss as a result of light scattering from scattering center defects in the SiO_2 is, in general, completely negligible. However, a few of the integral coverslip cells produced have exhibited these scattering centers while remaining acceptable in all other aspects. Loss even in these extreme cases has not exceeded 1%.

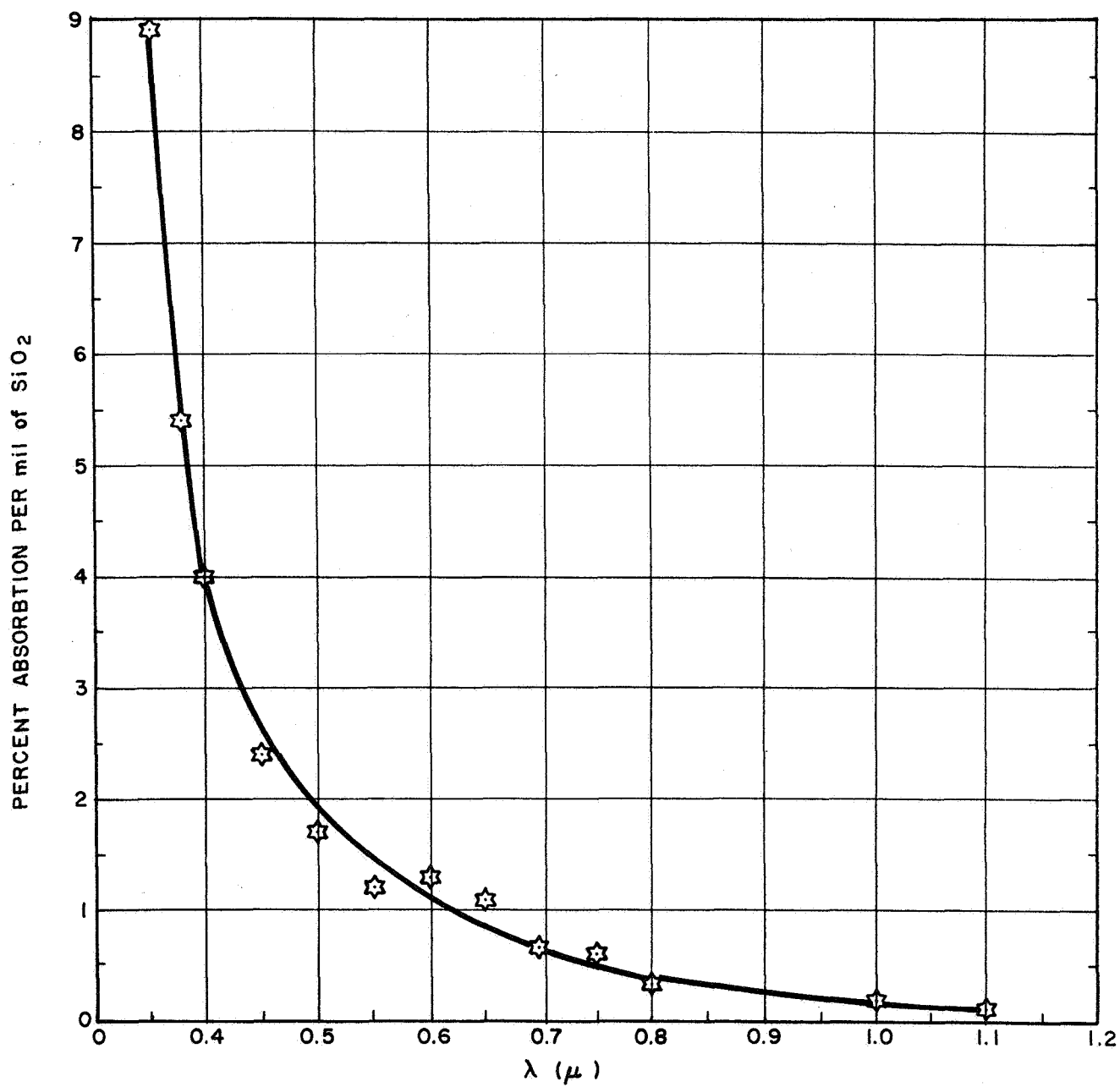


Figure 12. Absorption per mil of High Vacuum Sputtered SiO₂ as a Function of Wavelength

SECTION 5

FUTURE PLANS

Work will continue on deposition techniques for producing thick integral coverslips. In addition to high vacuum sputtering, RF and dc sputtering investigations will be continued. These techniques will also be applied to Al_2O_3 , as well as SiO_2 .

Analysis of the strain exhibited in the deposited material and techniques to reduce the strain and/or accompanying stress in the silicon will be investigated. Use of Al_2O_3 instead of SiO_2 may also lead to an overall strain reduction.

Testing of the cells with integral coverslips will be continued as required by the work statement.

PRECEDING PAGE BLANK NOT FILMED.

SECTION 6

REFERENCES

- (1) Brenner, A. and Senderoff, S., J. Res. N.B.S., Vol. 42, 105 (1949).
- (2) Runyan, W. R., "Silicon Semiconductor Technology", pp 220-221, McGraw-Hill (1965).
- (3) Oswald, R. B., IEEE Trans. Nuc. Sci., Vol. NS-13, 6, 63 (1966).
- (4) Progress Report No. 1, Contract NAS5-10319, Texas Instruments Incorporated, Dallas, Texas.
- (5) Janus, A. R. and Shrin, G. A., J. Vac. Sci. Tech. 4, 37 (1967).

DISTRIBUTION LIST

<u>Addressee</u>	<u>Copies</u>
NASA-Goddard Space Flight Center Greenbelt, Maryland 20771 Attention:	
Office of the Director - Code 100	1
Office of the Assistant Director for Administration and Technical Services - Code 200	3
Office of the Assistant Director for Projects - Code 400	1
Office of the Assistant Director for Systems Reliability - Code 300	1
Office of the Assistant Director for Tracking and Data Systems - Code 500	1
Office of the Assistant Director for Space Sciences - Code 600	1
Office of the Assistant Director for Technology - Code 700	1
GSFC Library - Code 252	2
Contracting Officer - Code 247	1
Technical Information Division - Code 250	4
Technical Representative - Code 716	25
NASA Headquarters FOB 10B Washington, D. C. 20546 Attn: Arvin Smith, Code RNW	1
Anderson, Donald NASA/Ames Research Center Moffett Field, California	1
Bachner, Robert L. Solar Systems, Inc. 8241 N. Kimball Avenue Skokie, Illinois 60078	1

<u>Addressee</u>	<u>Copies</u>
Baicker, J. A. Princeton Research and Development Company Box 641 Princeton, New Jersey	1
Barkley, Dwight W. Liberty Mirror, L. O. F. Brackenridge, Pennsylvania 15014	1
Brancato, E. L. N. R. L. Washington, D. C.	1
Chamberlin, R. R. National Cash Register Company Main and K Streets Dayton, Ohio	1
Cherry, William R. NASA/Goddard Space Flight Center Greenbelt, Maryland 20771	1
Cole, Robert L. Texas Instruments Dallas, Texas	1
Cusano, Dominic A. General Electric, R&D Center P. O. Box 1088 Schenectady, New York	1
Dawson, John R. NASA/Langley Research Center Langley Station Mail Stop 188-B Hampton, Virginia 23365	1
Downing, R. G. TRW Systems 1 Space Park Redondo Beach, California	1
Fang, P. H. (Dr.) NASA/Goddard Space Flight Center Greenbelt, Maryland 20771	1

<u>Addressee</u>	<u>Copies</u>
Ferguson, George D. (Jr.) General Electric Carroll Avenue Lynchburg, Virginia	1
Finger, Harold B NASA Headquarters Washington, D. C. 20546	1
Fischell, Robert JHU/Applied Physics Laboratory Silver Spring, Maryland	1
Hamilton, Robert C. Institute for Defense Analyses 400 Army-Navy Drive Arlington, Virginia 22202	1
Hawkins, Kenneth D. Ryan Aeronautical Company Lindberg Field San Diego, California 92112	1
Haynes, Gilbert A. NASA/Langley Research Center Langley Station Hampton, Virginia 23365	1
Holloway, H. Philco Research Laboratory Blue Bell, Pennsylvania	1
Hood, John Dow Corning Corporation Hemlock, Michigan 48626	1
Iles, Peter A. Hoffman Electronics Corporation 4501 Arden Drive El Monte, California	1
Jilg, Eugene T. Communications Satellite Corporation 2100 L Street, N. W. Washington, D. C. 20037	1

<u>Addressee</u>	<u>Copies</u>
Johnson, Carl E. Bellcomm, Inc. 1100 17th Street, N. W. Washington, D. C.	1
Julius, Richard F. Keltec Industries, Inc. 5901 Edsall Road Alexandria, Virginia 22314	1
Kaye, S. Electro-Optical Systems Inc. 300 No. Halstead Street Pasadena, California	1
King, W. J. (Dr.) Ion Physics Corporation Burlington, Massachusetts 01803	1
Kittl, Emil U. S. Army Electronics Command Attn: AMSEL-KL-PA Fort Monmouth, New Jersey CC-07703	1
Kling, Harry P. Hittman Associates Beltimore, Maryland	1
Loferski, Joseph J. (Dr.) Brown University Providence, Rhode Island	1
Marks, Burton S. Lockheed Missile and Space Company Palo Alto, California	1
Massie, Lowell D. AF Aero Propulsion Laboratory APIP-2 Wright-Patterson Air Force Base, Ohio	1
Mlavsky, A. I. (Dr.) Tyco Laboratories, Inc. Bear Hill Waltham, Massachusetts 02154	1

<u>Addressee</u>	<u>Copies</u>
Mott, James L. Fairchild Hiller Corporation Rockville, Maryland	1
Oman, Henry Boeing Company Seattle, Washington 98166	1
Pearson, Gerald L. Stanford University Stanford, California	1
Potter, Andrew NASA/Lewis Research Center 21000 Brookpark Road Cleveland, Ohio 44135	1
Plauche, Fulton M. NASA/Manned Space Flight Center EP-5 Houston, Texas 77058	1
Ralph, E. L. Heliotek 12500 Gladstone Avenue Sylmar, California	1
Rappaport, Paul RCA Laboratories Princeton, New Jersey	1
Ray, Kenneth A. Hughes Aircraft Company El Segundo, California	1
Reynard, Duncan L. Philco WOL Palo Alto, California	1
Riel, Robert K. Westinghouse Electric Corporation Semiconductor Division Youngwood, Pennsylvania 15697	1

<u>Addressee</u>	<u>Copies</u>
Ritchie, Donald W. Jet Propulsion Laboratory Pasadena, California	1
Schach, Milton NASA/Goddard Space Flight Center Greenbelt, Maryland 20771	1
Schaefer, James C. Harshaw Chemical Company 1945 E. 97th Street Cleveland, Ohio	1
Schlotterbeck, R. S. General Electric Company Lynchburg, Virginia	1
Schwarz, F. C. NASA/ERC 575 Technology Square Cambridge, Massachusetts 02139	1
Shirland, F. A. Clevite Corporation 540 E. 105th Street Cleveland, Ohio 44108	1
Slifer, Luther W. (Jr.) NASA/Goddard Space Flight Center Greenbelt, Maryland	1
Timberlake, Allen B. Battelle Memorial Institute 505 King Avenue Columbus, Ohio 43201	1
Waddel, Ramond C. (Dr.) NASA/Goddard Space Flight Center Greenbelt, Maryland 20771	1
Winkler, Seymour H. RCA/AED P. O. Box 800 Princeton, New Jersey 08540	1

<u>Addressee</u>	<u>Copies</u>
Wise, Joseph F. USAF-APL APIP-2 Wright-Patterson Air Force Base Dayton, Ohio	1
Yannoni, Nicholas F. AF Cambridge Research Laboratories L. G. Hanscom Field Bedford, Massachusetts 01731	1
Wolf, Martin RCA/AED Princeton, New Jersey	1
Marinozzi, D. Optical Coating Laboratories Santa Rosa, California	1
Starkey, Gerald E. (Major) Headquarters USAF AFRSTD Pentagon Washington, D. C.	1
Werth, John J. General Motors Defense Research Laboratories 6767 Hollister Avenue Goleta, California	1